



17 October 1997

**CHEMICAL
PHYSICS
LETTERS**

Chemical Physics Letters 277 (1997) 456–464

Bifurcation diagrams of periodic orbits for unbound molecular systems: FH_2

M. Founargiotakis^{a,b}, S.C. Farantos^{a,b}, Ch. Skokos^c, G. Contopoulos^c

^a *Institute of Electronic Structure and Laser, Foundation for Research and Technology, Hellas, Greece*

^b *Department of Chemistry, University of Crete, Iraklion, Crete 711 10, Greece*

^c *Department of Astronomy, University of Athens, Panepistimiopolis, Zographou, Athens 15783, Greece*

Received 23 May 1997; in final form 14 August 1997

Abstract

We present bifurcation diagrams of periodic orbits for the collinear FH_2 reactive system. The principal families which originate from the van der Waals minima and the saddle point are connected with a number of saddle node bifurcations. Saddle node bifurcations also emerge in the area of the saddle point of the potential function with periodic orbits which bridge the region between reactant and product channels. These saddle node bifurcations appear in a regular pattern with their critical energies of generation converging to a limiting value. Each successive saddle node bifurcation contains periodic orbits which increase by one the number of turning points in the reactant channel. © 1997 Elsevier Science B.V.

1. Introduction

The investigation of spectroscopy and dynamics of small polyatomic molecules has been a subject of research for decades. However, the study of excited molecules at high vibrational levels has only recently been pursued with new experimental techniques [1] and progress in theoretical methods [2]. Conceptual advances were born by studying low and high resolution spectra and interpreting spectroscopy with time-domain theories which involve the propagation of wave packets [3,4]. Spectroscopic features resulting from non-linear effects can easily be understood as due to the localization of wave packets in configuration space. On the other hand, reactive systems are of particular interest for understanding elementary chemical processes and they usually form a separate field of study [5]. The use of spectroscopic and

scattering techniques has been imposed by the nature of the molecular quantum states encountered in the different energy regimes, i.e. bound states are mainly studied with spectroscopic methods and unbound states are explored by scattering techniques. However, important dynamical effects in reactive systems, such as quantum resonances, are explained by using unbound states with a high degree of localization in configuration space.

The progress of non-linear classical mechanics has helped to elucidate a lot of spectroscopic characteristics of vibrationally highly excited molecules which behave as non-linear systems. Particularly, the periodic orbit analysis of small polyatomic molecules has proved to be a powerful tool for interpreting and predicting the spectroscopy and dynamics of these multidimensional systems [6]. After the pioneering works of Gutzwiller [7–9] and Heller [10,11] a corre-

spondence between periodic orbits (POs) and quantum mechanical wavefunctions has been shown. Most of the work in molecules has been done for bound states. The first association of periodic orbits with molecular states in unbound systems was made in the case of FH_2 [12,13]. Later, Davis and coworkers [14,15] extended this for a number of collinear reactions.

Bound systems offer more favorable conditions than unbound ones for a comparison of classical and quantum mechanics, since the strong mixing regime in phase space is gradually approached from the harmonic regime which is valid at low energies. Furthermore, the availability of spectroscopic data allows comparisons with experiment [16].

New experimental techniques have allowed spectroscopy in the area of the transition state of reactive systems to be done. A prototype reaction of this kind is [17,18]



for which the photoelectron spectroscopy of the stable negative ion FH_2^- has revealed a number of reaction resonances.

The first interpretation of the reaction resonances in terms of periodic orbits came from Pollak and Child [12]. These authors distinguished the periodic orbits crossing the entrance and exit channels of the potential surface from the periodic orbits which are located in the transition region. They called the first “periodic orbit dividing surfaces” (PODS) and the second class “resonant periodic orbits” (RPO). More recently, Hahn and Taylor [19], stimulated by the photoelectron experiments of Weaver and Newmark [17] have located new RPOs which they call “exchange” POs instead of “resonant periodic orbits”. They also use the term “in-channel” orbits instead of PODS. All the periodic orbits that they found were in a 2-dimensional coordinate space, since they were restricted to the plane of the two stretching modes without any bending motion.

New experimental results from the Newmark group [18] have stimulated more theoretical work in an effort to reproduce the photoelectron spectra and the reaction cross sections [20]. Russell and Manolopoulos [21] solved the time-dependent Schrödinger equation and calculated a high resolution spectrum for this system. These investigators

have also extracted the eigenfunctions of a few resonances and they separate them into reactant resonances, direct scattering states and product resonances.

We have been using the periodic orbits in a systematic way to study the spectroscopy and dynamics of triatomic and tetratomic molecules [6]. An outcome of this work is to establish a correspondence between the POs and the quantum mechanical wavefunctions. With *systematic work* we mean the construction of bifurcation diagrams by varying the total energy of the molecule. This procedure reveals the way that the POs emerge and how their stability changes with the energy. A number of interesting phenomena have been discovered such as the quantum manifestation of complex instability [22] and the importance of saddle node bifurcations for molecular systems [23]. However, all of the previous research has been done for bound systems. We feel that our strategy can be applied to unbound molecular systems for a better understanding of reaction resonances. The purpose of this Letter is to carry out a systematic study of the periodic orbit structure of FH_2 , especially in the transition state region. In spite of all the previous work to associate resonances to periodic orbits no systematic work has been presented up to now for this prototype reactive molecular system.

2. Computational details

In the history of $\text{F} + \text{H}_2$ as a prototype for testing new theoretical methods in computing reaction probabilities, the ground electronic state has been described with several potential functions. As is always the case, different potentials satisfy partially the experimental data. Among the most successful potential functions are the 5SEC [24] and the T5a [25] which have been used in quantum mechanical scattering calculations. Recently, a new potential was produced by Stark and Werner [26] based on extended ab initio calculations.

In the present work we have used the 5SEC [24] potential energy surface. We have chosen this function since it was available to us and allows us to compare with the work of Hahn and Taylor [19]. Our aim is to carry out a qualitative study of the families

of POs which are born in this type of potential function. Generally, we do not expect significant changes in the behaviour of the principal families of periodic orbits when the main topographical characteristics of the PES do not change.

For collinear geometries the 5SEC potential supports two minima: one is the van der Waals minimum in the reactant channel ($F + H_2$) with $R_{FH} = 5.4448 a_0$, $R_{HH} = 1.4 a_0$ and an energy -0.000669 hartree and the other in the $H + HF$ product channel with the geometry, $R_{FH} = 1.733 a_0$, $R_{HH} = 4.668 a_0$ and an energy -0.051105 hartree. The barrier that separates these two minima is at $R_{FH} = 3.170 a_0$, $R_{HH} = 1.437 a_0$ and at an energy 0.002507 hartree. The energy is measured with respect to reactants and with the hydrogen molecule at its equilibrium bond length.

The calculations which mainly involve the solution of the classical Hamilton equations of motion are performed by using scaled Jacobi coordinates. The Jacobi coordinates are the distance of fluorine atom from the center of hydrogen molecule, R , the distance of hydrogen molecule, r , and the angle between the vectors \mathbf{R} and \mathbf{r} , θ . The scaled coordinates are produced by defining the parameter

$$\alpha = \left[\frac{2m_H + m_F}{4m_F} \right]^{1/4}, \quad (2)$$

and the new coordinates are

$$sR = R/\alpha, \quad sr = ar, \quad s\theta = \theta. \quad (3)$$

Periodic orbits have been located by simple shooting methods and their continuation has been done by varying the total energy of the system. The theory and the algorithms have been reviewed extensively in previous publications [27].

3. Results and discussion

A systematic search for periodic orbits requires first the location of the principal families of periodic orbits which originate from the stationary points of the potential. According to the Weinstein [28] and Moser [29] theorems we expect at least as many principal families as the number of degrees of freedom.

Another category of important POs are the saddle nodes [30] (SN). These families appear suddenly in phase space at certain energies with two branches simultaneously; one branch with stable POs and one with unstable POs. The importance of SN bifurcations stems from the fact that the generation of stable POs brings order in regions of phase space even where chaotic trajectories exist at lower energies.

Fig. 1 presents contours of the potential function on which the stationary points of the surface are marked. These are two minima, one in the reactant channel for $F-H_2$ (\square) and one in the product channel for $H-HF$ (\circ) and the saddle point (\triangle) which separates the two minima. The thick line which passes through the stationary points is a curve defined by the equation

$$\exp[-50(sr - 1.05)] + 0.9508sr - sR + 2.39 = 0. \quad (4)$$

This curve is not exactly the minimum energy path but Eq. (4) has been used to define a Poincaré surface of section in our search for periodic orbits. This type of Poincaré surface of section is useful because the periodic orbits we are seeking are localized in different regions of the potential (in the reactant or product channel) and the commonly defined Poincaré planes of sections are no longer adequate.

We have located periodic orbits with no bending motion. We expect from the minima two families of periodic orbits which correspond to the stretching modes of the system. One of them describes motions leading to the dissociation of the molecule, and the other perpendicular motions towards the hard walls of the potential (see Fig. 1). The latter are important because they survive up to high energies and they have been associated with the in-channel resonances [19]. From the saddle point we expect one stretching family of periodic orbits which is unstable because of the unstable directions which lead to the reactant and product channels. It is interesting to see the bifurcation diagrams of these principal families shown in Fig. 2. We plot the sR coordinate of the initial conditions of periodic orbits with the energy. We denote the principal families with a number to distinguish the two different minima and a letter which distinguishes the branches bifurcating from

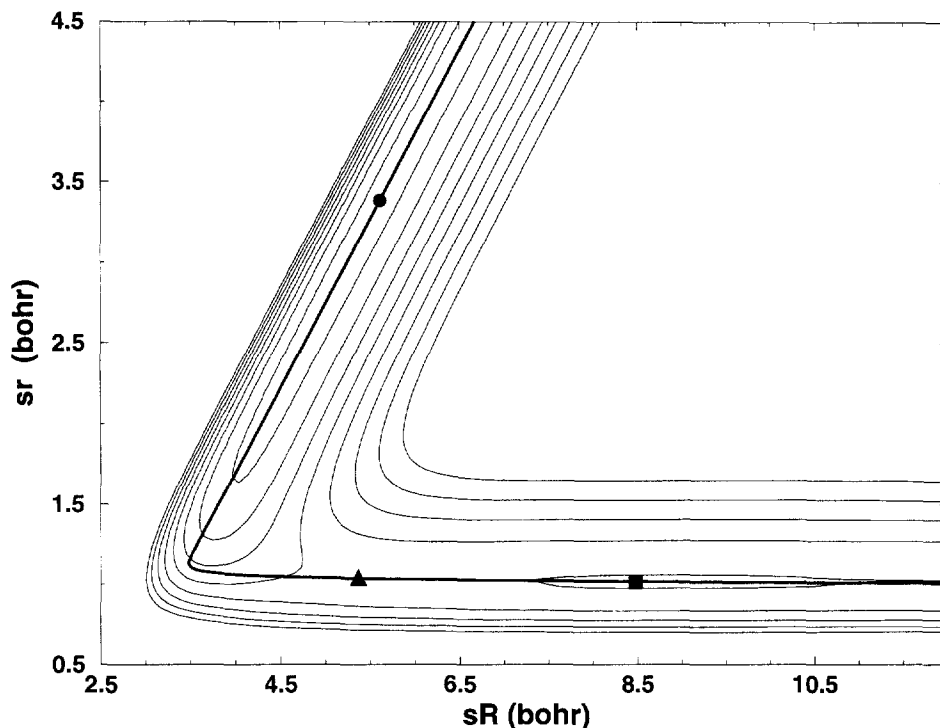


Fig. 1. Potential energy contours for collinear geometries of FH_2 in scaled Jacobi coordinates. The minimum energy contour is -0.045 hartree and the energy step for the contours is 0.015 hartree. The symbols \circ , \square and \triangle denote the positions of the two minima and the saddle point.

the principal families. New families of periodic orbits emerging from previous bifurcations may be denoted in a similar way with a second number and letter (e.g. $1c1a$). The $1sn1a$ family shown in Fig. 2 is a bifurcation of a saddle node periodic orbit.

One observation is that the bifurcation line that starts from the minimum of the reactant channel (orbits 2) ends at the saddle point of the potential after giving rise to a number of saddle node bifurcations, branches 2a, 2b, 2c and 2d. We may say that the branch 2c and the principal family which originates from the saddle point, 2d, are the two branches of a saddle node bifurcation which occurs at about 0.16 hartree and extend to smaller energies (reverse saddle node bifurcation).

The stability of the periodic orbits changes every time the line passes through a minimum or maximum of the energy. In fact, the stability of the periodic orbits changes more frequently as the energy increases and new periodic orbits bifurcate ev-

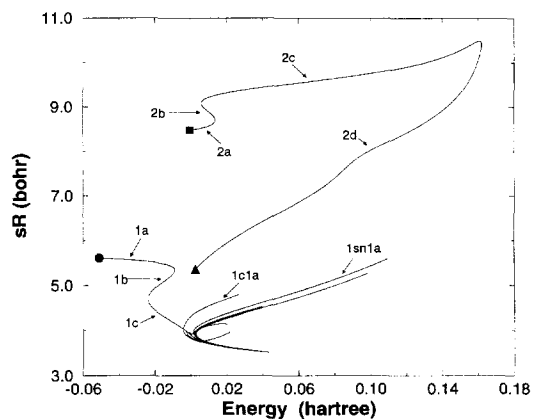


Fig. 2. Bifurcation diagram for the principal families of FH_2 which originate from the stationary points of the potential function. 1a is the principal family emanating from the product channel, 2a from the reactive channel and 2d from the saddle point. The letters a, b, c, and d are used to distinguish different bifurcation branches.

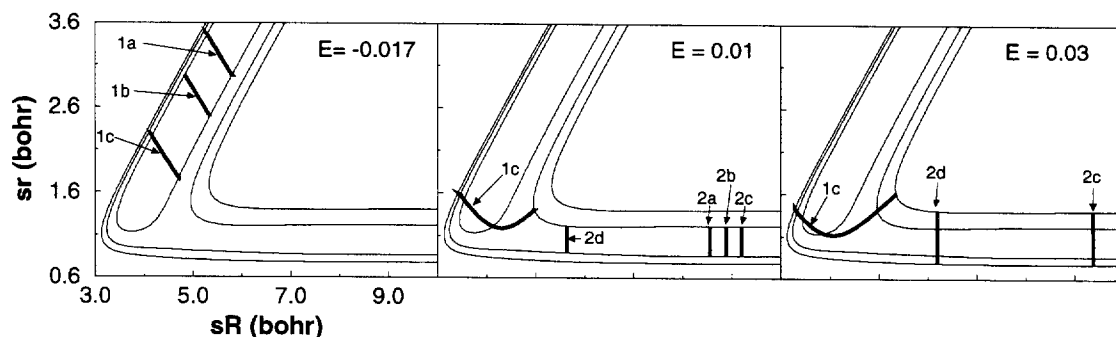


Fig. 3. Representative periodic orbits of the principal families and their bifurcations at several energies. Energy in hartree. Due to the appearance of minima and maxima with energy in the bifurcation curves at specific energies more than one POs may exist, i.e. 1a, 1b, and 1c at $E = -0.017$ hartree.

ery time the stability of the principal family alters. However, the morphology of these periodic orbits does not change and all of them correspond to PODS [13] or in-channel periodic orbits [19]. Representative POs of the principal families are shown in Fig. 3. We can see in this figure that for certain energy intervals periodic orbits of all branches co-exist.

The principal family that originates from the minimum of the product channel (orbits 1) passes through a minimum and a maximum energy as in the case of the reactant channel. It extends above the saddle point of the potential but it shows a rich bifurcating structure in the area of the saddle point of the potential. As we can see from Fig. 3 the morphology of these periodic orbits changes drastically for energies higher than the potential barrier and they approach the area of saddle point. Notice, however, that these periodic orbits always remain in the configuration region of the product channel in spite of the amount of energy they have.

The bifurcating families from the 1c branch produce periodic orbits of higher multiplicity. The 1c1a and 1sn1a POs emerge with a period doubling. The 1c1a are circular type orbits, i.e. without turning points. The triple and higher order periodic orbits show the oscillatory behaviour of the saddle node POs in the product channel as we shall see later on. These bifurcating families have a branch with periodic orbits which go away from the saddle point and penetrate deeper in the product channel with an increase in energy. This can be seen in the bifurcation diagram of Fig. 2. For example the 1c1a and

1sn1a branches show an increase of the sR coordinate with the total energy.

Pollak et al. [31] in their study of $F + H_2$ system with the Muckerman V potential surface [32] present periodic orbits of multiplicity one which show similar behaviour with an increase in the energy, i.e. they go away from the saddle point and inside the product channel. These periodic orbits are what they call PODS in the product channel. The authors did not construct bifurcation diagrams but it is quite probable that these periodic orbits are bifurcations of the principal family of the product channel. We could not find bifurcating periodic orbits of simple multi-

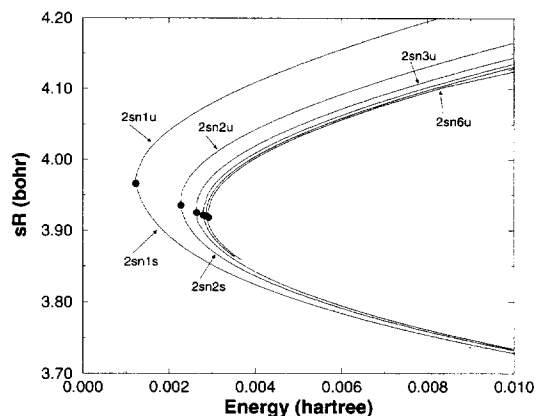


Fig. 4. Bifurcation diagram for the saddle node periodic orbits in the transition state region. The symbols $2snis$ and $2sniu$ denote the stable and unstable periodic orbits of the i th saddle node bifurcation which oscillate in the reactant channel.

Table 1

Energies E , periods T and initial conditions for the saddle node periodic orbits at the energy of their generation; i denotes the number of turning points of the POs in the reactant channel (see text)

i	E (hartree)	T ^a	sR ^b	sr	$ P_{sR} $	$ P_{sr} $
1	0.001271	951.787366	3.983211	1.675653	9.841151	8.197512
2	0.002274	1387.488332	3.939691	1.629881	9.938584	8.085914
3	0.002639	1762.688887	3.930259	1.619961	9.973659	8.070882
4	0.002800	2124.600797	3.926313	1.615810	9.989099	8.064821
5	0.002877	2480.482723	3.924546	1.613953	9.996552	8.062553
6	0.002917	2833.635795	3.923658	1.613018	10.000323	8.061409

^a One atomic time unit corresponds to 2.419×10^{-17} s.

^b Distances in a_0 .

plicity for the 5SEC potential function in the range of energies we examined. Nevertheless, even the higher multiplicity POs will act as PODS since they act as dynamical barriers for the reactive trajectories.

The third category of periodic orbits we have located are the saddle nodes. Fig. 4 presents six saddle node bifurcations and in Table 1 we tabulate the energies, periods and the initial conditions (coordinates and momenta) of the periodic orbits at their generation point. As we mentioned above, at the critical energy where the SN bifurcation emerges, two families of periodic orbits appear, one stable and one unstable. In the bifurcation diagrams of the SN families we label the two branches as **2snis** and **2sniu** for the stable and unstable branch respectively, and $i = 1, 2, \dots, 6$. The stable periodic orbits turn to unstable with a small increase in the energy. That is why we do not use different types of lines for the

two branches as is customary. The periods of the POs of a SN bifurcation increase with the energy for the **2snis** branch and decrease for the **2sniu** branch. This trend of periods turns out to be a general characteristic of the saddle node bifurcations [6].

The morphologies of the SN POs are shown in Fig. 5 at an energy of 0.0035 hartree. These periodic orbits bridge the two regions of the potential, the reactant and product valley, and show an increasing oscillatory behaviour in the reactant channel with the appearance of new SN bifurcations. According to the number of the turning points in the reactant channel we label the SN bifurcations with $i = 1, 2, \dots, n$. Note, the different morphology of the periodic orbits in the two branches for a specific SN bifurcation. Although both the **2snis** and **2sniu** have similar sr values in the reactant channel they have different sr values in the product channel; the **2snis** PO ends at a

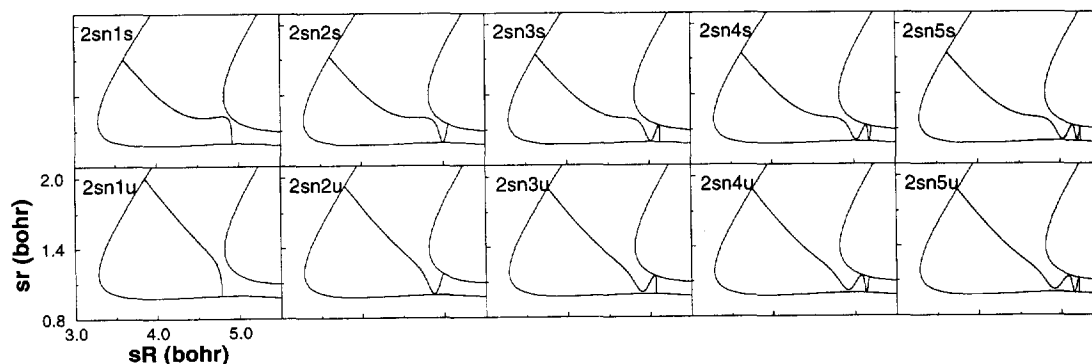


Fig. 5. Representative periodic orbits of saddle node type at the energy of 0.0035 hartree.

lower sr value than the 2nd PO. With increasing energy the SN POs penetrate deeper and deeper into the reactant channel.

The first two SN bifurcations occur at critical energies below the energy of the potential barrier and inside the product valley. Also, from Fig. 4 we can see that the origins of the SN bifurcations seem to converge to a limiting energy. Indeed, we have tried to model the generation energies of the SN periodic orbits by fitting their initial conditions to simple polynomials of the total energy E , thus hoping to predict higher order SN bifurcations. The fitted functions are:

$$sR = 10938.0E^2 - 81.8294E + 4.06953 \quad (5)$$

$$sr = 11504.1E^2 - 86.0642E + 1.76644 \quad (6)$$

$$P_{sR} = 96.7492E + 9.71827 \quad (7)$$

$$P_{sr} = 43275.8E^2 - 263.2490E + 8.46211, \quad (8)$$

where P_{sR} and P_{sr} are the conjugate momenta to sR and sr respectively. The periods of the SN POs at the critical energies of their generation are well fitted by a linear function;

$$T = 372.861i + 618.434, \quad i = 1, \dots, 6. \quad (9)$$

Using Eqs. (5)–(8) we have tried to produce initial conditions to locate the generation point of the SN bifurcations of higher multiplicity. Unfortunately, this scheme did not work satisfactorily. Starting with the predicted initial conditions our program could not converge to the new SN bifurcation.

A more successful approach was obtained when we modeled the differences of the initial conditions of POs at a particular energy, E . We found that the differences of the ratios

$$d = \frac{\delta_{j,i}}{\delta_{j,i+1}} - \frac{\delta_{j,i+1}}{\delta_{j,i+2}}, \quad (10)$$

where

$$\delta_{j,i} = x_{j,i} - x_{j,i+1}, \quad (11)$$

and $x_{j,i}$ are the initial conditions ($j = 1, 2, 3, 4$) of the i th SN periodic orbit, can be modeled with exponential functions of the form

$$d = A \exp(-\beta i). \quad (12)$$

This method allowed us to locate periodic orbits of higher order for a specific energy using the data from the POs of lower order to fit the parameters A and β of Eq. (12). In Table 2 we give initial conditions for SN POs of order $i = 1 - 9$ at the energy 0.008 hartree.

The ratios $\frac{\delta_{j,i}}{\delta_{j,i+1}}$ tend to the same limit for all initial conditions ($j = 1, 2, 3, 4$) when $i \rightarrow \infty$, although the values $\delta_{j,i}$ are different. The limit depends only on the energy E ; e.g. for $E = 0.008$ hartree this limit is 0.78. The generation of such saddle node bifurcations seems to be a more general phenomenon, since, they have also been found for bound molecular potentials [6,16] and other dynamical systems [33].

Table 2

Initial conditions for the saddle node periodic orbits at an energy of 0.008 hartree; i denotes the number of turning points of the POs in the reactant channel; A and β are the fitted parameters in Eq. (12) (see text)

i	T^a	sR^b	sr	$ P_{sR} $	$ P_{sr} $
1	821.985082	4.195593	1.899025	10.447844	9.404767
2	1206.149216	4.131454	1.831567	10.455187	9.280855
3	1570.132402	4.110916	1.809966	10.457659	9.233523
4	1925.909606	4.102147	1.800744	10.458724	9.212026
5	2277.688335	4.097929	1.796307	10.459238	9.201395
6	2627.329272	4.095768	1.794034	10.459501	9.195874
7	2975.764939	4.094620	1.792827	10.459641	9.192920
8	3323.499475	4.093996	1.792171	10.459717	9.191309
9	3670.818677	4.093652	1.791809	10.459759	9.190419
A		0.614948	0.614832	0.586157	0.412399
β		0.535727	0.535675	0.528194	0.490153

^a One atomic time unit corresponds to 2.419×10^{-17} s.

^b Distances in a_0 .

The number of these saddle node bifurcations is infinite. The appearance of infinite saddle node bifurcations in dynamical systems is due to Birkoff's theorem [34] which secures the existence of infinite periodic orbits near homoclinic and heteroclinic points. Newhouse [35] has studied the phenomenon of the generation of saddle node bifurcations when the stable and unstable manifolds of unstable periodic orbits touch one another.

The oscillatory behaviour of SN POs leads one to the conclusion that the origin of these saddle node bifurcations is the unstable periodic orbits 2d, something which is difficult to show with numerical calculations. It is therefore tempting to ask if similar series of SN POs exist in the product channel. We found periodic orbits which oscillate in the product channel but they have their origin in the bifurcating families of the 1c branch of the principal family in the product valley. However, saddle node series could appear at any region of configuration space. We believe that the most important are those which are associated with the unstable POs of saddle points of the potential function, since this region of configuration space is significant for reactive scattering. A systematic search for locating periodic orbits should include this region.

POs have been used to trace the localization of the eigenfunctions in configuration space. For unbound systems this is equivalent to associating periodic orbits to quantum resonances. Russell and Manolopoulos [21] have carried out time-dependent quantum mechanical calculations using the Stark–Werner potential function. Having obtained a resolution of 1 meV in the calculated photoelectron spectrum they managed to assign and plot the wavefunctions which correspond to several peaks in the spectrum. A number of these wavefunctions carry bending excitation. In Fig. 3 of their Letter they show the wavefunctions which correspond to the first three peaks of their spectrum for collinear para-FH₂. The nodal patterns of the wavefunctions are given in the (*sR*, *sr*) plane. What Russell and Manolopoulos name in their Letter as reactant and product resonances (their Figs. 3(a) and 3(c)) can be associated with the principal periodic orbits 2 and POs localized in the product channel. However, the wavefunction which they assign as a direct scattering state, (their Fig. 3(b)), shows appreciable amplitude in the configura-

tion space where the three colliding atoms are in close proximity as well as in regions inside the product channel. The saddle node periodic orbits (Fig. 5) can justify the observed localization of the wavefunction for small *sr* and *sR* values.

4. Conclusions

We have carried out a periodic orbit analysis of a typical reactive chemical system, FH₂, using a previously used potential function. From the bifurcation diagrams we have concluded:

(1) The principal families originate in the van der Waals minima of the reactant and product channels and at the saddle point between these two minima. Their bifurcation diagrams show minima and maxima with the energy which are saddle node bifurcations.

(2) A branch of the principal family which emanates from the reactant channel (2c) and the principal family which emanates from the saddle point (2d) are the two branches of an inverse saddle node bifurcation which emerges at high energy.

(3) The principal family which originates from the minimum of the product channel extends above the saddle point of the potential through the generation of a few branches of saddle node bifurcations. A number of multiple period periodic orbits bifurcate from the branch 1c which penetrate in the product channel with the increase of the energy.

(4) The saddle node bifurcations which originate below and above the saddle point of the potential are generated in a regular fashion by successively increasing the number of turning points in the reactant channel.

Acknowledgements

We are glad to acknowledge financial support from the General Secretariat for Research and Technology (Grant No. PENED 89E Δ86).

References

- [1] H.-L. Dai, R. Field (Eds.), *Molecular Dynamics and Spectroscopy by Stimulated Emission Pumping*, World Scientific, Singapore, 1995.

- [2] R. Kosloff, *Ann. Rev. Phys. Chem.* 45 (1994) 145.
[3] E.J. Heller, *Acc. Chem. Res.* 14 (1981) 368.
[4] E.J. Heller, in: *Chaos and Quantum Physics*, M. Giannoni, A. Voros, J. Zinn-Justin (Eds.), Elsevier, Amsterdam, 1991.
[5] R.D. Levine, R.B. Bernstein, *Molecular Reaction Dynamics and Chemical Reactivity*, Oxford University Press, Oxford, 1987.
[6] S.C. Farantos, *Internat. Rev. Phys. Chem.* 15 (1996) 345.
[7] M.C. Gutzwiller, *Chaos in Classical and Quantum Mechanics*, vol. 1, Springer, Berlin, 1990.
[8] M.C. Gutzwiller, *J. Math. Phys.* 8 (1967) 1979.
[9] M.C. Gutzwiller, *J. Math. Phys.* 12 (1971) 343.
[10] E.J. Heller, *Phys. Rev. Letters* 53 (1984) 1515.
[11] P. O'Connor, J. Gehlen, E.J. Heller, *Phys. Rev. Letters* 58 (1987) 1296.
[12] E. Pollak, M.S. Child, *Chem. Phys.* 60 (1981) 23.
[13] E. Pollak, in: M. Baer (Ed.), *Theory of Chemical Reaction Dynamics*, vol. 3, CRC, Boca Raton, FL, 1985, p. 123.
[14] M.J. Davis, *J. Chem. Phys.* 86 (1987) 3978.
[15] R.T. Skodje, M.J. Davis, *J. Chem. Phys.* 88 (1988) 2429.
[16] S.C. Farantos, H.-M. Keller, R. Schinke, K. Yamashita, K. Morokuma, *J. Chem. Phys.* 104 (1996) 10055.
[17] A. Weaver, D.M. Neumark, *Faraday Discussions Chem. Soc.* 91 (1991) 5.
[18] S.E. Bradforth, D.W. Arlond, D.M. Neumark, D.E. Manolopoulos, *J. Chem. Phys.* 99 (1993) 6345.
[19] O. Hahn, H.S. Taylor, *J. Chem. Phys.* 96 (1992) 5915.
[20] J.F. Castillo, D.E. Manolopoulos, K. Stark, H.-J. Werner, *J. Chem. Phys.* 104 (1996) 6531.
[21] C.L. Russell, D.E. Manolopoulos, *Chem. Phys. Lett.* 256 (1996) 465.
[22] G. Contopoulos, S.C. Farantos, H. Papadaki, C. Polymilis, *Phys. Rev. E* 50 (1994) 4399.
[23] S.C. Farantos, *Laser Chem.* 13 (1993) 87.
[24] G.C. Lynch, R. Steckler, D.W. Schwenke, A.J.C. Varandas, D.G. Truhlar, B.C. Garrett, *J. Chem. Phys.* 94 (1991) 7136.
[25] R. Steckler, D.G. Truhlar, B.C. Garrett, *J. Chem. Phys.* 82 (1985) 5499.
[26] K. Stark, H.-J. Werner, *J. Chem. Phys.* 104 (1996) 6515.
[27] S.C. Farantos, *THEOCHEM J. Mol. Struct.* 341 (1995) 91.
[28] A. Weinstein, *Inv. Math.* 20 (1973) 47.
[29] J. Moser, *Comm. Pure Appl. Math.* 29 (1976) 727.
[30] J. Guckenheimer, P. Holmes, *Nonlinear Oscillations, Dynamical Systems, and Bifurcations of Vector Fields*, Springer, Berlin, 1983.
[31] E. Pollak, M.S. Child, P. Pechukas, *J. Chem. Phys.* 72 (1980) 1669.
[32] G.D. Schatz, J.M. Bowman, A. Kuppermann, *J. Chem. Phys.* 63 (1975) 674.
[33] G. Contopoulos, *Celest. Mech.* 24 (1981) 355.
[34] G.D. Birkoff, *Acta Math.* 50 (1927) 359.
[35] S.E. Newhouse, *Publ. Math. IHES* 50 (1979) 101.